Remote Sensing of Environment 114 (2010) 950–960

Contents lists available at ScienceDirect

Remote Sensing of Environment

journal homepage: www.elsevier.com/locate/rse

Comparison and evaluation of Medium Resolution Imaging Spectrometer leaf area index products across a range of land use

Francis Canisius [a,*], Richard Fernandes [a], Jing Chen [b]

[a] Canada Centre for Remote Sensing, 588 Booth St., Ottawa, Ontario, Canada K1A 0Y7
[b] University of Toronto, 100 George St., Toronto, Ontario, Canada M5S 3G3

ARTICLE INFO

Article history:
Received 8 April 2009
Received in revised form 11 December 2009
Accepted 12 December 2009

Keywords:
MERIS
LAI
Validation

ABSTRACT

Leaf area index (LAI) is a commonly required parameter when modelling land surface fluxes. Satellite based imagers, such as the 300 m full resolution (FR) Medium Spectral Resolution Imaging Spectrometer (MERIS), offer the potential for timely LAI mapping. The availability of multiple MERIS LAI algorithms prompts the need for an evaluation of their performance, especially over a range of land use conditions. Four current methods for deriving LAI from MERIS FR data were compared to estimates from in-situ measurements over a 3 km × 3 km region near Ottawa, Canada. The LAI of deciduous dominant forest stands and corn, soybean and pasture fields was measured in-situ using digital hemispherical photography and processed using the CANEYE software. MERIS LAI estimates were derived using the MERIS Top of Atmosphere (TOA) algorithm, MERIS Top of Canopy (TOC) algorithm, the Canada Centre for Remote Sensing (CCRS) Empirical algorithm and the University of Toronto (UofT) GLOBCARBON algorithm. Results show that TOA and TOC LAI estimates were nearly identical (R^2>0.98) with underestimation of LAI when it is larger than 4 and overestimation when smaller than 2 over the study region. The UofT and CCRS LAI estimates had root mean square errors over 1.4 units with large (~25%) relative residuals over forests and consistent underestimates over corn fields. Both algorithms were correlated (R^2>0.8) possibly due to their use of the same spectral bands derived vegetation index for retrieving LAI. LAI time series from TOA, TOC and CCRS algorithms showed smooth growth trajectories however similar errors were found when the values were compared with the in-situ LAI. In summary, none of the MERIS LAI algorithms currently meet performance requirements from the Global Climate Observing System.

1. Introduction

Leaf Area Index (LAI) is defined as one half the total green leaf (more generally foliage) area per unit horizontal ground surface area (Chen & Black, 1992). The Global Climate Observing System (GCOS) has identified LAI as an essential climate variable given its role in regional and global carbon, energy and water cycle models (GCOS, 2006). GCOS has specified a requirement for global daily ~250 m resolution LAI estimates with a total error of less than 10%.

A number of regional and global studies have assessed the accuracy of LAI estimates from moderate (>250 m) resolution satellite sensors (Morisette et al., 2006; Weiss et al., 2007; Garrigues et al., 2008a). Garrigues et al. (2008a) documented sources of uncertainty including: (1) acquisition noise due to detector quality, point spread function (PSF) corresponding to the reference, calibration errors, atmospheric and cloud contamination, background, topography, view-illumination geometry and saturation; (2) canopy related parameters such as clumping, mixed pixel, variations in understory, woody matter and leaf structure; and (3) accuracy of secondary data input (e.g., aerosol optical depth, land cover). A common finding in many of the LAI validation studies is the variability in accuracy as a function of land cover (e.g. Bacour et al., 2006; Abuelgasim et al., 2006; Yang et al., 2006; Houborg et al., 2007). The variability can be caused by uncertainties of land cover specification in the case of algorithms that directly require land cover as an input (Cohen et al., 2003) or biases in priori assumptions regarding controls on reflectance for a given land cover class during algorithm calibration (Yang et al., 2006). Fernandes et al. (2004) found that one third of the error in their LAI estimate was due to mixing of land cover classes within a 1 km pixel. In comparison, MERIS offers a nearly 10 fold reduction in pixel footprint that may minimize the land cover mixture effect. However, MERIS spectral sampling is restricted to visible and near infrared wavelengths where sensitivity of top of canopy reflectance to leaf biochemistry and understory conditions may be substantial (Delegido et al., 2008; Canisius & Chen, 2007) and atmospheric correction relative uncertainties may be large for dark targets (Fernandes et al., 2004). It is therefore critical to determine how well existing MERIS LAI algorithms perform over a variety of land cover types typically found in a single global biome.

* Corresponding author.
E-mail address: Francis.Canisius@NRCan.gc.ca (F. Canisius).

0034-4257/$ – see front matter.
doi:10.1016/j.rse.2009.12.010

LAI estimates are now available based on various operational algorithms (Baret et al., 2006a,c; Deng et al., 2006; and in this study using the approach of Fernandes et al., 2003) originally designed for application to a range of multi-spectral moderate resolution imagers and applied to 300 m resolution data from the Medium Resolution Imaging Spectrometer (MERIS FR) on board the ENVISAT satellite. The goal of this paper is to assess the agreement of LAI products generated from four operational algorithms using the same input MERIS FR data to in-situ based estimates over a region where coincident in-situ LAI estimates are available. Intercomparison of MERIS LAI products from all four algorithms is also performed. Further, this study analyzed the seasonal temporal consistency of LAI for different land use types derived using selected algorithms from multi temporal MERIS FR data sets.

2. Methods

2.1. Study area and field data collection

The study area was located in Nepean (45:18 N, 75:45 W), Ottawa, Canada (Fig. 1). Corn, soybean, wheat and pasture were the main agriculture practices in the study area. The agriculture fields were uniformly planted within each field using a fixed spacing by crop type and a standard site preparation. Most of the agriculture fields were rectangular in shape with an average size of 20 ha. Low density deciduous dominant mixed forest tracts were also present in isolated patches as well as a larger tract in the South East of the study area shown in Fig. 1. Intensive field campaigns for in-situ LAI estimation were performed three times in summer 2006 but a clear sky MERIS image was only available close to the second visit (04–05 July 2006) so we will only discuss about the in-situ data collected during that visit. For the 04–05 July 2006 field campaign 35 elementary sampling units (ESUs) from 19 agriculture fields were selected a priori to include replicate land cover samples. Eight ~1 ha forest ESUs were selected a priori to span the expected range in forest LAI based on a nominal forest LAI estimate derived from a summer 2006 Landsat 5 Thematic Mapper image following the approach of Butson & Fernandes (2004). A limited evaluation of temporal consistency of MERIS LAI estimates within the growing season was performed with repeated DHP based LAI estimates over a corn (CFIA_05) field and a soybean (CFIA_16) field during 2008 growing season following the methodology for in-situ survey used with the 2006 in-situ estimates described below.

For agricultural fields, ESU were surveyed using digital hemispherical photographs (DHP) on two parallel 60 m transects along planted rows, separated by 50 m to allow for an estimate of within field variability. Line transects have been long advocated and tested for indirect LAI estimation over row crops (LI-COR, 1992.; Welles & Cohen, 1996) and have been successfully used at our study area in the past based on comparison to destructive sampling (Strachan et al., 2005). For each transect 13 DHPs were taken (Fig. 2a). Seven DHPs were acquired 10 m apart, starting at the transect origin, with azimuth

Fig. 1. Study site located in Nepean area (45:18 N, 75:45 W) Ottawa, Canada (sharpened false color image of July 30, 2006 Landsat TM scene).

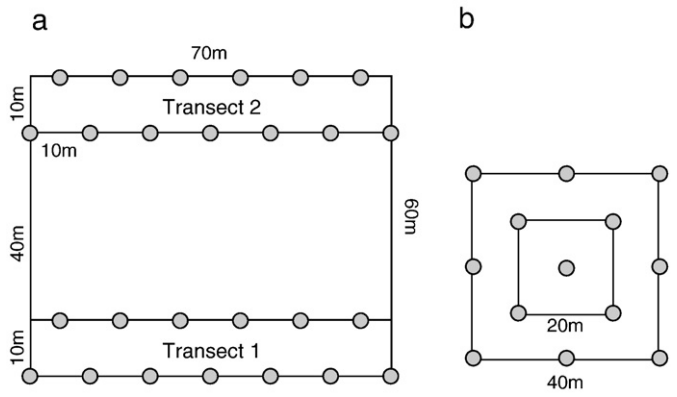

Fig. 2. DHP elementary sampling units (ESUs), (a) crop field transects, (b) forest nested box.

oriented randomly in the quadrant aligned with the transect. A further 6 DHPs, 10 m apart, were acquired returning to the transect origin oriented in azimuth randomly in the quadrant perpendicular to the transect. The DHPs were acquired using Nikon CoolPix 8800 cameras with Nikon FC-E9 Fisheye adapter at full 8 Mb pixels Nikon Exchange Format to preserve radiometric data without scaling (Nikon Co., 2006). Upward looking images were acquired when non-woody vegetation was at least 50 cm above ground level. Otherwise downward looking images were acquired with a minimum distance between lens and target of twice the maximum foliage element dimension as recommended in LI-COR (1992). Digital DHPs were acquired on June 4th and 5th, 2006 under clear sky conditions with manual adjustment of exposure and f-stop settings to avoid signal saturation. DHPs were also acquired over the forest ESUs using the VALERI nested box (Fig. 2b) sampling method (Morisette et al., 2006) that includes 13 upward (canopy) and downward (understory) samples forming nested boxes around each plot centre. Manual exposure and aperture settings were used for upward looking images following Chen et al. (2006) while automatic settings were used for downward images after Garrigues et al. (2008b).

In-situ LAI estimates were derived from the 13 DHPs of each transect (or nested box) in an ESU using the CAN_EYE version 3.6 software (http://www.avignon.inra.fr/can_eye, Garrigues et al., 2008b; and Demarez et al., 2008). Manual masking of the solar disk, dark shadows, trunks or broad woody stalks and areas of specular reflection was performed in all DHPs. Gap fraction is calculated from the RGB images through a supervised classification using 5° zenith and 5° azimuth discretization restricted to a zenith range of 0° to 60° as in Garrigues et al., 2008b and Demarez et al., 2008. CANEYE estimates effective LAI (L_e) by model inversion based on a Poisson model, where the foliage is assumed randomly distributed (Weiss et al., 2004). The LAI is related to L_e through the clumping index (Chen & Black, 1992), which depends on canopy structure, foliage distribution and size and shape of leaves (Chen et al., 2005). CAN_EYE uses Lang's logarithm gap fraction averaging method (Lang & Xiang, 1986) to estimate clumping. The 5° discretization allows for capturing changes in clumping with zenith angle but may also result in a bias compared to other methods for estimating clumping from DHP images (Leblanc et al., 2005). Recent work suggests that this bias may not be as significant (<10%) for crops (Demarez et al., 2008) and broadleaf forests (Leblanc et al., 2005) in comparison to orchards (López-Lozano et al., 2009).

LAI estimates were quality controlled by examining diagnostics including the modeled versus observed gap fraction, the estimated clumping index as a function of zenith angle, and the deviation between effective LAI estimated by the multiple zenith angle estimate of Weiss et al. (2004) and from 5° zenith angle range centered at 57.5° zenith angle. The latter is a necessary condition that the observed gap fractions are generated by statistical arrangements of vegetation that meet the modified Poisson distribution required by the Nilson (1971) theory that forms the basis of CANEYE L_e estimation.

Image based reference LAI map was produced by assigning average of ESU estimates to the polygon area of each agriculture field and by developing and applying a simple ratio (near infrared/red hemispherical directional reflectance) versus LAI transfer function over 30 m forest pixels using a Landsat 5 Thematic Mapper (TM5) image acquired on 30th July 2006. The linear transfer function was developed by using the average 3×3 TOA reflectances at each of the eight forest ESUs and applying a robust to measurement error regression (Butson & Fernandes, 2004). The goal of the transfer function design for the forested regions was to provide an unbiased rather than precise LAI estimate since upscaling the 30 m Landsat scale LAI fields to 300 m MERIS pixels should minimize most random errors. The 30 m reference LAI map was upscaled by overlaying with the nominal MERIS pixel grid.

2.2. MERIS LAI estimation

A single MERIS FR Level 1P top-of-atmosphere radiance product (Table 1), corresponding to a nominal local acquisition time of 10:35, July 3, 2006, was used for the spatial comparison of LAI in our study. The lack of additional images during our 2006 growing season was primarily due to the limited capacity for systematic archiving of MERIS FR imagery over North America prior to April, 2008. Twelve

Table 1
Data used for the evaluation.

Date	MERIS data	MODIS aerosol products
2006		
07-03-2006	MER_FR__1PNUPA20060703_153356_000000982049_00097_22696_0052.N1	MOD04_L2.A2006184.1535.005.2006205174129.hdf
2008		
06-12-2008	MER_FRS_1PNPDK20080612_151928_000004582069_00240_32859_3210.N1	MOD04_L2.A2008164.1635.005.2008165152331.hdf
06-15-2008	MER_FRS_1PNPDK20080615_151841_000005352069_00283_32902_3827.N1	MOD04_L2.A2008167.1530.005.2008168163550.hdf
06-21-2008	MER_FRS_1PNPDK20080621_153106_000004502069_00369_32988_5756.N1	MOD04_L2.A2008173.1630.005.2008174163508.hdf
06-25-2008	MER_FRS_1PNPDK20080625_150922_000004332069_00426_33045_6687.N1	MOD04_L2.A2008177.1605.005.2008178175407.hdf
07-01-2008	MER_FRS_1PNPDK20080701_151650_000005352070_00011_33131_8924.N1	MOD04_L2.A2008183.1530.005.2008184190522.hdf
07-07-2008	MER_FRS_1PNPDK20080707_152812_000005372070_00097_33217_0763.N1	MOD04_L2.A2008189.1630.005.2008190063333.hdf
07-17-2008	MER_FRS_1PNPDK20080717_151405_000005352070_00240_33360_3458.N1	MOD04_L2.A2008199.1530.005.2008200104632.hdf
08-14-2008	MER_FRS_1PNPDK20080814_153355_000005352071_00140_33761_0439.N1	MOD04_L2.A2008227.1555.005.2008233100534.hdf
08-18-2008	MER_FRS_1PNPDK20080818_150821_000005352071_00197_33818_2074.N1	MOD04_L2.A2008231.1530.005.2008235232856.hdf
08-20-2008	MER_FRS_1PNPDK20080820_154517_000005352071_00226_33847_2672.N1	MOD04_L2.A2008233.1515.005.2008236104352.hdf
08-21-2008	MER_FRS_1PNPDK20080821_151403_000005352071_00240_33861_2854.N1	MOD04_L2.A2008234.1600.005.2008237001228.hdf
08-27-2008	MER_FRS_1PNPDK20080827_152522_000005352071_00326_33947_4317.N1	MOD04_L2.A2008239.1620.005.2008240140416.hdf

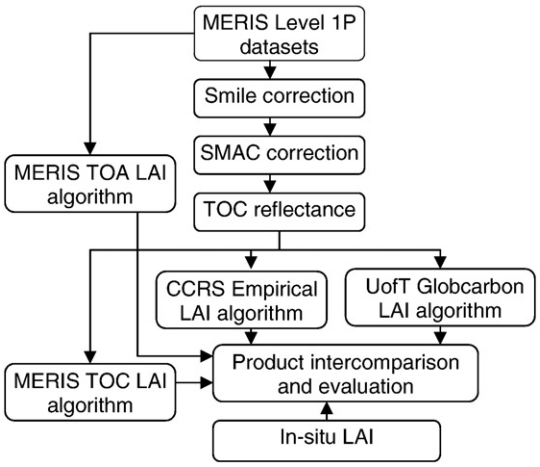

Fig. 3. Steps of MERIS LAI comparison and evaluation.

cloud free MERIS FRS images (Table 1) were acquired by direct reception over Canada during the growing season of 2008 to evaluate the temporal consistency of MERIS LAI estimates. MERIS images were processed from Level 0 to Level 1P by the European Space Agency using their MERIS instrument processing facility (IPF) processor. Level 1P images were subsequently processed to top of canopy reflectance at Canada Centre for Remote Sensing using standard tools in the BEAM Toolbox (http://www.brockmann-consult.de/beam/downloads.html). The outline (Fig. 3) presented here shows the steps of MERIS Level 1P data processing to estimate LAI and the comparison and evaluation of estimated LAI with in-situ measurements.

MERIS Level 1P images were reprojected to the same projection (WGS 84) and coordinate system (UTM 18) as the LAI reference image (in-situ LAI) and resampled using nearest neighbor interpolation. The geometric accuracy of the MERIS Level 1P images were evaluated manually, using the river network of an orthorectified Landsat 5 TM image (root mean square error for July 3, 2006 image was 103 m Easting and 87 m Northing). Level 1P TOA radiance images were converted to TOC reflectance images using the Simplified Method for Atmospheric Correction (SMAC) model (Rahman & Dedieu, 1994) within BEAM (http://www.brockmann-consult.de/beam/doc/help/). Ozone, water vapor and atmospheric pressure were derived from the MERIS Level 1P data. Aerosol optical thickness of each image was taken from the MODIS aerosol product (Table 4) derived from MODIS swath (Kaufman et al., 1997) acquired within a few minutes difference from MERIS acquisition (1 min difference for July 3, 2006 image). In addition to the collected in-situ land use information used for field specific LAI estimates, a land cover map of Canada 2005 (Latifovic et al., 2005), derived from 250 m MODIS data was used as input when producing regional LAI maps for two of the four algorithms.

Four operational LAI algorithms, described below, were applied to the TOA radiance or TOC reflectance image. Main characteristics and processing requirements of each LAI estimation algorithm is given in Table 2.

Table 2
Main characteristics and processing requirements of each LAI algorithm.

Characteristics and processing requirements	MERIS TOA LAI algorithm	MERIS TOC LAI algorithm	CCRS Empirical LAI algorithm	UofT GLOBCARBON LAI algorithm
Geometric correction	BEAM	BEAM	BEAM	BEAM
Datum	WGS 84	WGS 84	WGS 84	WGS 84
Projection	UTM 18	UTM 18	UTM 18	UTM 18
Resample	NN	NN	NN	NN
Pixel size	300 m	300 m	300 m	300 m
Smile Correction	MERIS TOA LAI algorithm	BEAM–Smile	BEAM–Smile	BEAM–Smile
Atmospheric correction and MERIS TOA radiance to TOC reflectance	MERIS TOA LAI algorithm	BEAM–SMAC	BEAM–SMAC	BEAM–SMAC
Ozone, water vapor and atmospheric pressure	Derived from MERIS data	Derived from MERIS data	Derived from MERIS data	Derived from MERIS data
Aerosol optical thickness	Derived from MERIS data	From MODIS aerosol product	From MODIS aerosol product	From MODIS aerosol product
Band normalization	N/A	N/A	Samain method	Samain method
From MERIS bands to SPOT VGT bands			665 nm to 657 nm 865 nm to 830 nm	665 nm to 657 nm 865 nm to 830 nm
Algorithms data Input	13 bands of MERIS TOA radiance, Solar and view angles	11 bands of MERIS TOC reflectance, Solar and view angles	Red (657 nm) and NIR (865 nm) TOC reflectance	Red (657 nm) and NIR (865 nm) TOC reflectance, Solar and view angles
Algorithm specifications				
Models	Coupled SMAC, SAIL and PROSPECT models	SAIL and PROSPECT models	Empirical NDVI, SR – LAI relationship	4_scale model derived SR – LAI relationship
Inversion	Neural network inversion	Neural network inversion	Empirical equations corn LAI $= 0.1505\ e^{3.9703\ NDVI}$ soybean LAI $= 0.0189\ e^{6.7273\ NDVI}$ pasture LAI $= -0.2075 + 0.2288$ SR forest LAI $= -0.021\ SR^2 + 0.9857$ SR $- 1.6788$	LUT inversion based on land cover 2005 map
Clumping representation				
Plant/shoot scale	N/A	N/A	Empirical samples	Clumping index map
Canopy scale	N/A	N/A	Empirical samples	Clumping index map
Landscape scale	Mixed pixels as fraction of pure vegetation or soil	Mixed pixels as fraction of pure vegetation or soil	Large sample size	N/A
Comments	Land cover independent, Easy to use	Land cover independent, MERIS image pre processing is required	Detailed land cover dependent, MERIS image pre processing is required	Land cover dependent, MERIS image pre processing is required
Reference	Baret et al. (2006c)	Bacour et al. (2006)	Fernandes et al. (2003)	Deng et al. (2006)

2.2.1. MERIS Top of Atmosphere (TOA) LAI algorithm

The TOA algorithm (Baret et al., 2006c) is based on inversion of coupled atmosphere (SMAC), canopy (SAIL, Verhoef, 1984) and leaf (PROSPECT, Jacquemoud & Baret, 1990) radiative transfer models given input MERIS TOA radiances. A neural network, trained with simulated TOA radiances in the 13 MERIS bands other than the oxygen (band 11) and water absorption (band 15) bands for a variety of land surface conditions, is used for inversion. The neural network once trained can be run in operational mode. BEAM software, MERIS TOA LAI algorithm ("TOA_VEG"), was used to estimate LAI from level 1P FR MERIS data (http://www.brockmann-consult.de/beam-wiki/display/BEAM/Plug-ins).

2.2.2. MERIS Top of Canopy (TOC) LAI algorithm

The TOC algorithm (Baret et al., 2006a; Bacour et al., 2006) relies only on the canopy-leaf (SAIL + PROSPECT) reflectance model simulated spectro-directional variation of the reflectance when training the neural network to estimate LAI from 11 bands of given MERIS TOC reflectance estimates. The first two shortest wavelength bands and the oxygen and water absorption bands have not been used in this approach assuming they would convey significant uncertainties associated while providing only marginal information on the surface (Baret et al., 2006a). The BEAM, MERIS TOC LAI algorithm ("TOC_VEG"), was used to estimate LAI from TOC reflectance data (http://www.brockmann-consult.de/beam-wiki/display/BEAM/Plug-ins).

2.2.3. The Canada Centre for Remote Sensing (CCRS) Empirical LAI algorithm

The CCRS algorithm allows estimation of LAI from vegetation indices (basically derived from SPOT VGT data) with land use/cover information and the appropriate empirical regression models (Fernandes et al., 2003). Thus, MERIS red (665 nm) and NIR (865 nm) bands were used to approximate SPOT VGT red (657 nm) and NIR (830 nm) bands respectively using the coefficients given in Samain (2006). Regression models (Fernandes et al., 2003) listed in Table 2 were used to estimate LAI for corn and soybean from NDVI and for grass and forest from simple ratio (SR). Normalization to the nominal 40° solar zenith angle and nadir view angle of the regression model was not applied since the solar and view angles of selected MERIS images are within the acceptable ranges (e.g. the July 3, 2006 MERIS overpass corresponded to a 29° solar zenith angle and the range of view zenith angles over our study site was between 3° and 5°).

2.2.4. The University of Toronto (UofT) GLOBCARBON LAI Algorithm

The 4Scale physically based geometrical optical model (Chen & Leblanc, 2001) is used to simulate the interaction between incoming solar radiation and the vegetated surface and thus to generate simulations relating LAI over an a priori range of ancillary parameters (e.g. soil and leaf optical properties, canopy shape and height) required to calibrate the UofT algorithm (Deng et al., 2006). LAI was derived based on the relationships between BRDF of Red and NIR bands and LAI for each of the major cover types using a large combination of these parameters with the use of LUT. Normalized MERIS red and NIR bands to SPOT VGT were used as input TOC reflectance. Required angular information about MERIS data for this algorithm was obtained from MERIS Level 1P data product. The algorithm also accounts for vegetation clumping at the plant and canopy scales by using the land cover dependent clumping index derived by Chen et al. (2005).

2.3. Selection of MERIS pixels for the evaluation

Evaluating LAI estimates from moderate resolution imagery is complicated by mixed pixels including sensitivity to adjacent regions due to the sensor projected instantaneous field of view (PIFOV), geolocation errors, and resampling (Fernandes et al., 2004; Weiss et al., 2007). Previous studies (Fernandes et al., 2004; Morisette et al., 2006) have simply aggregated satellite measurements over 3×3 pixels (or more) to minimize the PIFOV surface uncertainty when comparing to in-situ based reference estimates. This approach would prevent us from assessing LAI retrieval performance over individual land uses in our study area as none of the agriculture fields contained a 3×3 pixel region. Discarding fields not containing at least one MERIS FR pixel centered in the field would result in less than 10 MERIS FR pixels from the July 3, 2006 acquisition and thus substantially limit the precision of our intercomparison. As a practical compromise we selected MERIS pixels with reasonable overlap with a given field or within a forested region. The minimum permissible overlap for a pixel and a field to be used in LAI intercomparison was identified based on the maximum agreement rate between in-situ based and MERIS LAI estimates using all algorithms. This was typically encountered at a minimum overlap of ~75% since, as the minimum overlap level reached 100% outlier fields in terms of accuracy tended to positively bias the root mean square error (RMSE) LAI statistics while as the minimum overlap fall much below 75% the influence of adjacent fields on the MERIS LAI estimate reduced the overall LAI retrieval RMSE. Thirty six MERIS FR pixels that show more than 75% overlap during July 3, 2006 were selected for LAI intercomparison in this study. Four pixels corresponding to almost 100% overlap were used for the temporal assessment during 2008.

Blurring of the signatures due to the MERIS Point Spread Function (PSF) that consists of various components (listed in Zurita-Milla et al., 2007) may only slightly influence the actual reflectance of the

Table 3a
Reference in-situ average LAI values of agriculture fields (July 4–5, 2006).

Land use	Field name	Area (ha)	LAI	LAI range	Effective LAI	Effective LAI range
Soybean	Field CFIA_05	27.17	0.91	0.7–1.1	0.80	0.6–1.0
Soybean	Field GBF_13	21.38	1.03	0.9–1.1	0.80	0.8–0.8
Soybean	Field GBF_25E	28.11	0.85	0.4–1.0	0.66	0.4–0.9
Corn	Field CFIA_02	21.31	4.20	3.5–4.9	1.85	1.5–2.1
Corn	Field CFIA_03	22.45	2.95	2.5–3.4	1.70	1.6–1.8
Corn	Field CFIA_04	11.96	3.45	2.9–3.7	2.08	1.7–2.3
Corn	Field CFIA_06	28.16	4.27	3.6–5.2	2.08	1.9–2.3
Corn	Field CFIA_08	13.76	0.48	0.3–0.6	0.43	0.3–0.5
Corn	Field CFIA_09S	20.96	4.10	3.6–4.6	2.10	2.1–2.1
Corn	Field CFIA_11	24.06	3.97	3.6–4.4	2.20	2.0–2.5
Corn	Field CFIA_13	11.35	1.34	0.8–2.0	1.05	0.6–1.5
Corn	Field CFIA_14NE	14.73	5.55	4.5–6.9	3.55	3.2–3.8
Corn	Field CFIA_14	21.74	6.00	5.7–6.6	3.62	3.1–4.0
Corn	Field CFIA_15	17.44	4.55	4.4–4.7	2.70	2.6–2.8
Corn	Field CFIA_16	21.99	4.75	3.8–5.4	2.92	2.6–3.2
Pasture	Field CFIA_01	28.23	2.52	2.4–2.6	2.37	2.2–2.6
Pasture	Field CFIA_07	35.09	2.85	2.3–3.6	2.60	2.1–3.2
Pasture	Field CFIA_12	35.85	3.12	2.3–4.3	2.78	2.1–4.3
Pasture	Field CFIA_17	8.25	4.25	3.8–4.8	3.87	3.6–4.1

Table 3b
Reference in-situ LAI values of forest sampling units (July 4–5, 2006).

Forest type	Plot name	Area (ha)	LAI	LAI residual	Effective LAI	Effective LAI residual
Maple	Forest ESU_01	1	4.37	0.73	3.8	0.89
Alder/Maple	Forest ESU_03	1	4.02	0.45	3.6	0.75
Alder	Forest ESU_04	1	4.44	0.37	3.5	0.35
Maple/Pine	Forest ESU_05	1	5.42	0.01	3.5	0.83
Maple	Forest ESU_06	1	3.5	0.60	2.9	0.38
Alder	Forest ESU_07	1	4.26	0.72	3.0	0.17
Alder/Maple	Forest ESU_08	1	2.26	0.57	1.5	0.76
Alder/Maple	Forest ESU_09	1	2.3	0.37	2.0	0.13

Table 3c
Reference in-situ continues LAI values of corn and soybean fields (2008).

Date	Corn (CFIA_05)		Soybean (CFIA_16)	
	LAI	Effective LAI	LAI	Effective LAI
06-12-2008	Not surveyed	Not surveyed	0.16	0.20
06-20-2008	0.83	0.60	0.29	0.25
06-26-2008	2.05	1.15	0.64	0.49
07-03-2008	5.00	2.60	1.55	1.09
07-10-2008	5.85	3.95	3.30	2.35
07-17-2008	5.45	3.95	4.50	3.40
07-29-2008	5.80	3.95	6.85	4.30
08-18-2008	5.70	3.80	6.30	4.65
09-02-2008	4.05	2.75	Not surveyed	Not surveyed

selected MERIS FR pixels as the PIFOV of selected MERIS FR pixels are mostly centered within the homogenous spectral signature of the corresponding agriculture fields. Fields selected at the 75% overlap threshold typically included adjacent pixels within the same field on three of four sides so adjacency effects should also be minimized. Further, the sensitivity of residuals (RMSE) between MERIS and in-situ LAI to different resampling methods was less than 2% (relative).

3. Results and discussion

3.1. Reference field LAI

The in-situ LAI estimate of each agriculture field, for July 4–5, 2006, is given in Table 3a. In general the LAI range for an agriculture field was within 0.5 units indicating, as expected, that the fields were relatively uniform in LAI. For all crop ESUs except pasture, the Weiss et al. (2004) and 57.5° LAI estimates for each transect differed by less than the 0.5 units supporting the CANEYE theoretical assumptions and the adequacy of the spatial sampling within a sampling unit. The lower agreement over pasture was most likely due to insufficient gaps at 57.5º (the CANEYE software frequently reported annular segments with no gaps), even with <30 cm distance between lens and target, leading to noisy estimates of LAI from this zenith angle.

LAI estimation using CANEYE processed DHP's has been evaluated extensively elsewhere (Iiames et al., 2008; Garrigues 2008b; Chen et al., 2006; Demarez et al., 2008). Our in-situ measurements fall within the range of values cited in the literature from destructive sampling at this study area (Pattey et al., 2001) and other similar sites in North America (Wilhelm et al., 2000, Wiegand et al., 1990). Garrigues et al. (2008b) also found that the CANEYE/DHP approach provided robust and reasonable LAI estimates over soybean, corn and pasture land in Argentina using similar field sampling methods.

The forest LAI linear transfer function with 0.73 R^2 and 0.53 RMSE (based on leave-one-out cross validation) indicates the accuracy of the transfer function and its relevance for upscaling ESUs over the small forest tract in our study region. Table 3b shows the residual between the regression prediction and the LAI value of forest sampling unit (range 0.01 to 0.73) as an indicator of the prediction error of the spatial reference LAI estimates at 30 m resolution. Aggregation of the 30 m resolution forest LAI estimates to 300 m MERIS pixel footprints will reduce random components in this transfer function. As such, the 300 m scale in-situ forest LAI estimates

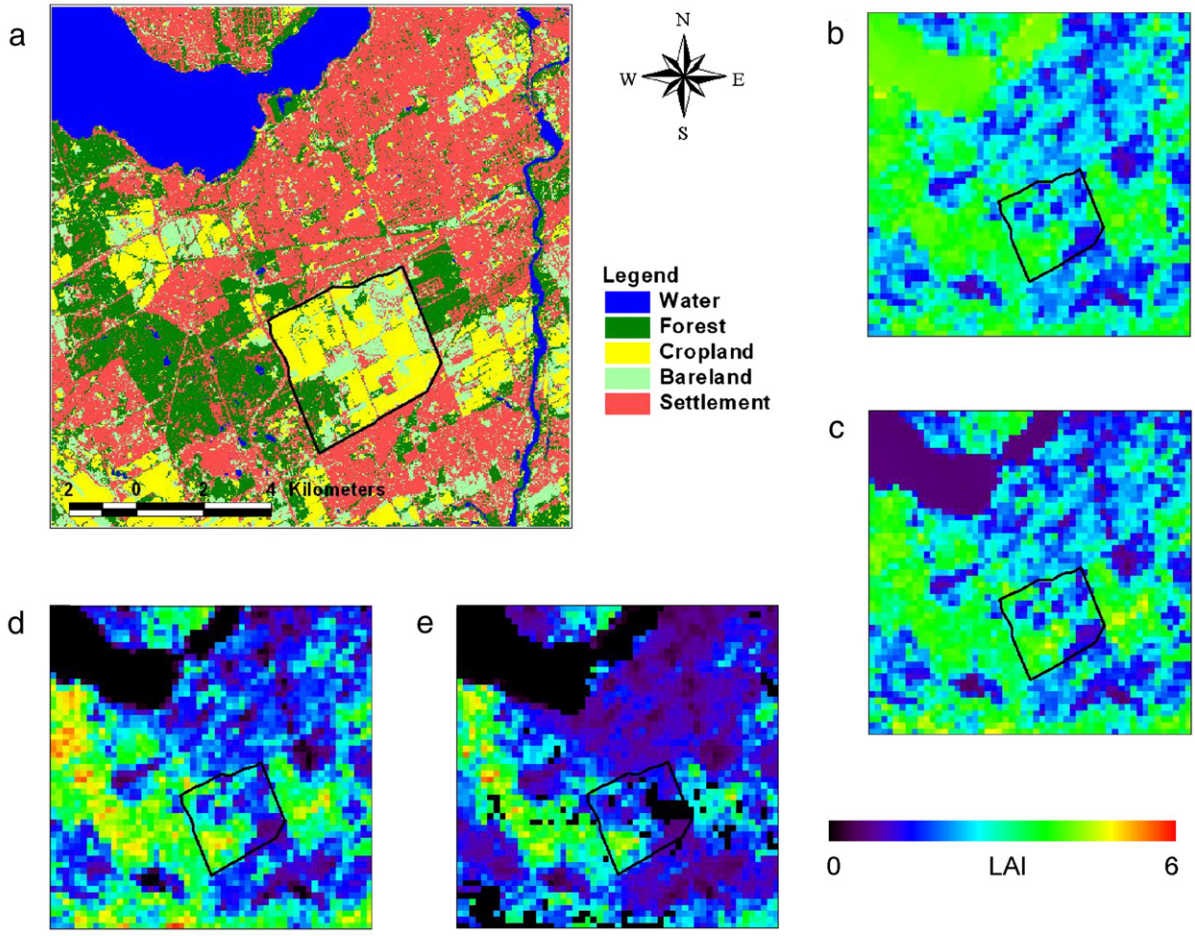

Fig. 4. (a) Main land covers of the study area (black polygon) and surrounding (July 2006 Landsat TM classification). (b) MERIS LAI image derived using TOA algorithm, (c) TOC algorithm, (d) CCRS algorithm and (e) UofT Algorithm.

may be substantially more precise than the 0.53 RMSE over the sampling unit.

Table 3c summarizes the temporal LAI estimates for the corn and soybean field surveyed during the 2008. The LAI values agree with published LAI trends over similar crops in North America (Wiegand et al., 1990; Pedersen & Lauer, 2004).

3.2. Evaluation of MERIS LAI products

3.2.1. Visual comparison

Fig. 4 shows the land cover of the study area and surrounding region, including Ottawa, Canada, together with the four different MERIS based LAI maps of that area for July 03, 2006. TOA and TOC LAI maps are very similar both in patterns and magnitudes of LAI. The CCRS LAI map has a similar pattern to the TOA and TOC LAI maps but shows larger values for forested regions to the south west of the study area. The UofT LAI map shows substantially lower values in the vicinity of regions already mapped as low LAI, typically urbanized regions rather than agriculture fields or forest, in the other three maps.

3.2.2. Comparison with in-situ LAI and L_e

Fig. 5 compares the in-situ (July 4–5, 2006) and MERIS (July 3, 2006) LAI estimates of 36 selected pixels over agriculture fields and the forest sites within the study area. Summary statistics regarding residuals between these two LAI values are given in Table 4. The RMSE values characterize the agreement between in-situ LAI and the MERIS LAI estimates. The observed RMSE values are larger than typical absolute uncertainties in the DHP based in-situ LAI estimates over agriculture fields (Demarez et al., 2008) and forest stands (Chen et al., 2006).

TOA and TOC LAI estimates show residuals within 1 LAI unit (RMSE of ~1 unit) and relatively small biases at low LAI levels. However, the larger (66%) TOA LAI and (42%) TOC LAI relative bias for open soybean fields suggests the influence of background on LAI estimation. Overall, both TOA and TOC algorithms clearly show saturation around in-situ LAI levels at or over four (see Fig. 5a and b) as reported in Bacour et al. (2006) and this saturation effect can also be seen in Fig. 4b and c. In comparison, the CCRS and the UofT LAI estimates show better agreement at low LAI levels but substantially larger land cover specific residuals (see Fig. 5c and d) at mid to high LAI levels (RMSE ~1.5). There is less evidence of saturation over high (>4) LAI forests with the CCRS and UofT LAI estimates in comparison to the TOA and TOC estimates. However residuals for forest pixels (see Fig. 5c and d) exhibit large variability for the CCRS and UofT algorithms. The CCRS LAI estimates also show a linear bias corresponding to an underestimate of ~40% for corn and pasture while the UofT LAI estimates exhibit large (>50%) outliers over 5 corn pixels.

The assumptions within the LAI algorithms regarding the clumping of vegetation as well as the ratio of woody to green area can impact LAI estimates (Garrigues et al., 2008a) and hence agreement with in-situ LAI. To diagnose some of this variability we also compared the MERIS LAI estimates with in-situ based L_e estimates for each algorithm (Fig. 6). The TOA and TOC LAI estimates have slightly lower RMSE (~0.9 vs ~1.0) but slightly large relative RMSE (~0.5 vs ~0.35) when compared against in-situ L_e versus in-situ LAI. Both algorithms do not show an obvious saturation level in the relationship between their LAI estimates and in-situ based L_e. The CCRS LAI algorithm shows

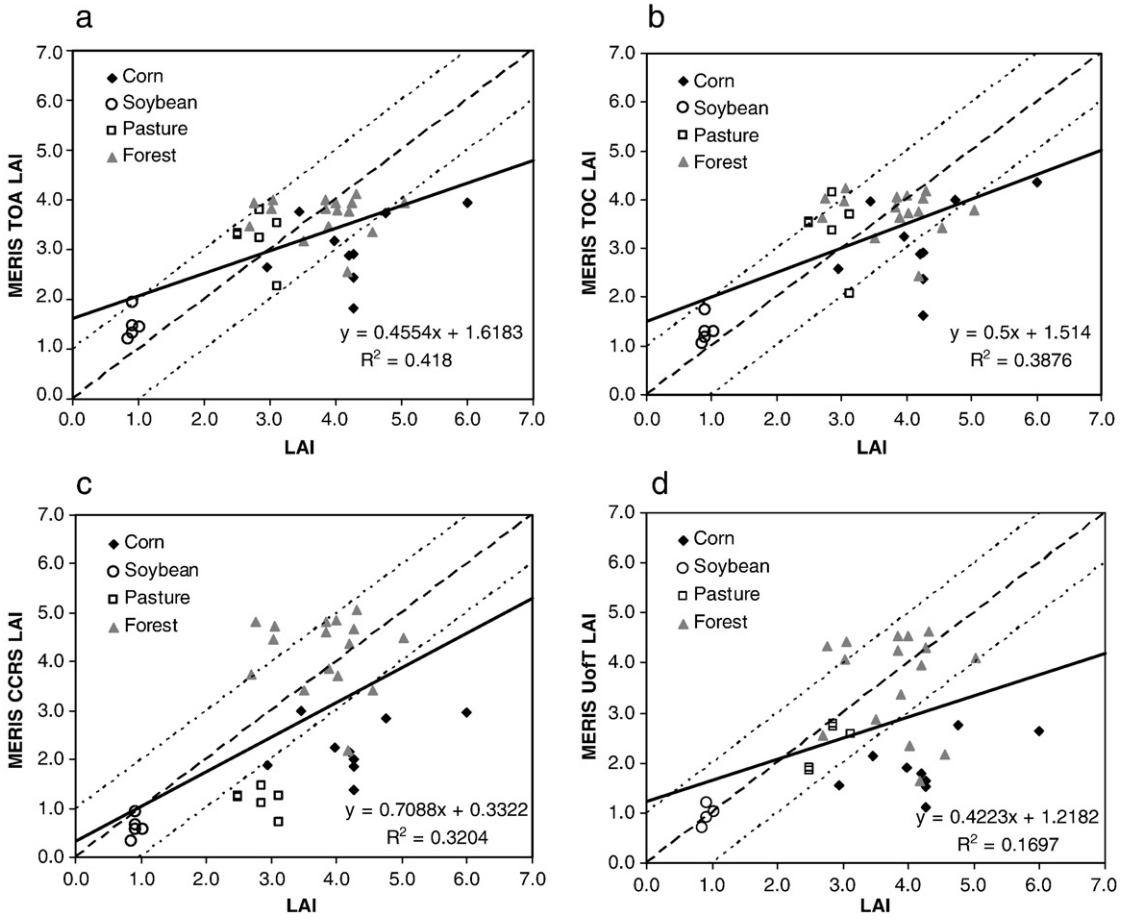

Fig. 5. Comparison between the in-situ LAI values to the corresponding LAI estimates from (a) TOA algorithm, (b) TOC algorithm, (c) CCRS algorithm and (d) UofT algorithm. Linear regression (solid line) and 1:1 line with ±1 unit range (dashed lines) are added.

Table 4
Root mean square error (RMSE) and relative RMSE (RRMSE) between MERIS LAI estimates and field LAI or effective LAI (L_e) estimates.

Landuse	Number of sample pixels	LAI	TOA LAI estimates		TOC LAI estimates		CCRS LAI estimates		UofT LAI estimates	
			RMSE	RRMSE	RMSE	RRMSE	RMSE	RRMSE	RMSE	RRMSE
All	36	LAI	0.96	0.34	1.00	0.33	1.47	0.43	1.51	0.37
		LAI_e	0.87	0.49	0.97	0.48	1.18	0.47	0.92	0.35
Corn	9	LAI	1.51	0.33	1.49	0.34	2.16	0.48	2.48	0.56
		LAI_e	0.88	0.43	0.99	0.46	0.49	0.22	0.57	0.23
Soybean	5	LAI	0.60	0.66	0.45	0.50	0.36	0.40	0.17	0.19
		LAI_e	0.73	0.93	0.57	0.72	0.23	0.31	0.23	0.29
Pasture	6	LAI	0.74	0.27	0.95	0.35	1.71	0.59	0.47	0.18
		LAI_e	0.85	0.33	1.07	0.42	1.46	0.55	0.35	0.15
Forest	16	LAI	0.77	0.22	0.84	0.24	1.09	0.33	1.20	0.32
		LAI_e	0.91	0.37	1.01	0.40	1.48	0.56	1.26	0.46

better agreement with L_e versus in-situ LAI for corn (RMSE drops from ~2 to ~0.5 for a reduction in relative RMSE over 50%) and no substantial change for pasture. The UofT LAI estimate shows strong agreement with L_e for all classes except forests where the scatter is similar to the LAI intercomparison reported in the previous paragraph. The TOA LAI algorithm agrees with in-situ based L_e (RMSE = 0.87) in comparison with the other algorithms.

3.2.3. MERIS LAI product intercomparison

We intercompared the spatial LAI estimates of each product to determine if the observed residuals over the limited reference targets were consistent with between product differences. Fig. 7a shows that the TOA and TOC LAI estimates were very strongly correlated ($R^2 = 0.99$) with the TOC estimates having a slight positive offset (0.3 units) and slope (1.1) in comparison to the TOA estimates. The offset could not be explained by reasonable (+/−0.1) adjustments in aerosol optical depth values which were estimated from 13 bands of MERIS image for MERIS TOA LAI algorithm and from MODIS aerosol product for MERIS TOC LAI algorithm.

CCRS LAI estimates and the UofT LAI estimates are correlated ($R^2 = 0.8$) over all cover classes except pasture (Fig. 7b). The strong correlations are due to the fact that both algorithms use indices derived from Red and NIR as their primary input. Differences over pasture are possibly due to the fact that the CCRS algorithm for this class is based on data from prairie grasslands rather than temperate short-grass pastures while the UofT algorithm relies on a radiative transfer model training data set with generic spectral and structural pasture characteristics.

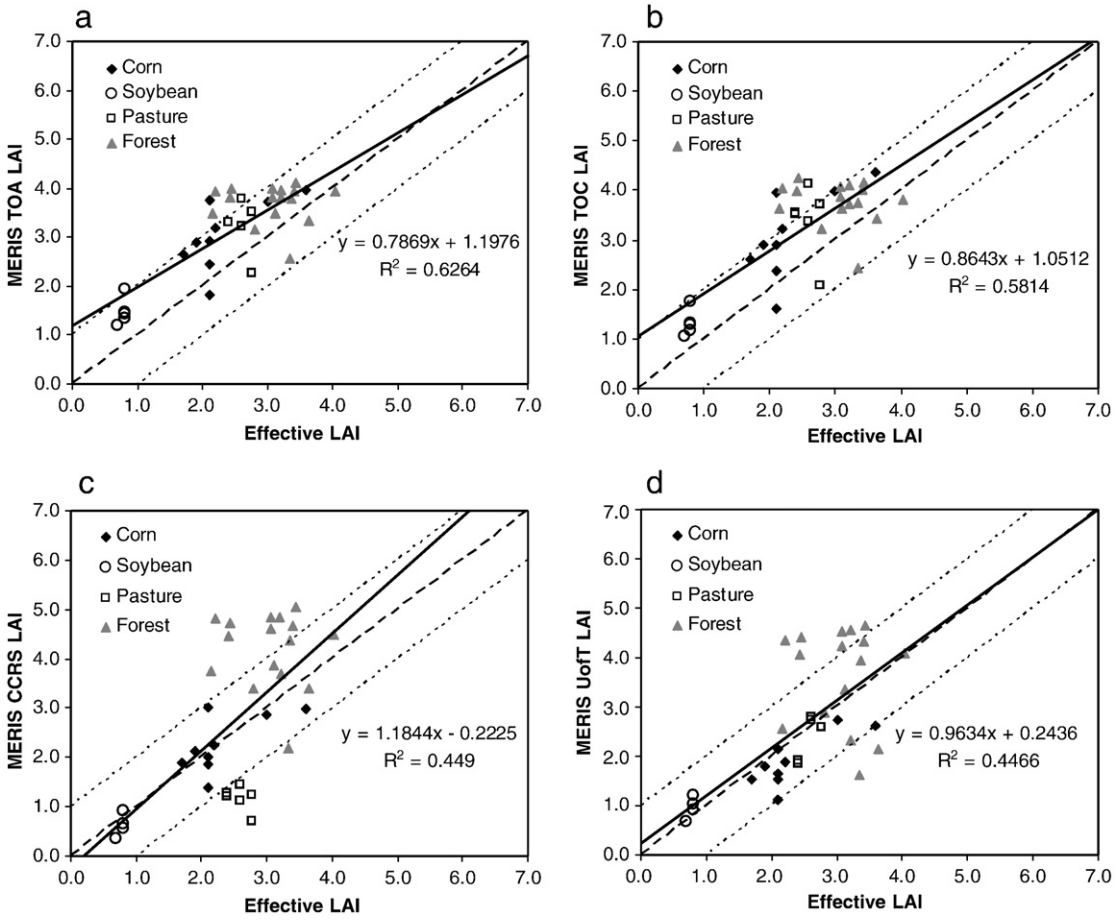

Fig. 6. Comparison between the effective LAI values derived from DHP ground measurements to the corresponding LAI estimates from each algorithm. Effective LAI vs (a) TOA LAI (b) TOC LAI (c) CCRS LAI and (d) UofT LAI. Linear regression (solid line) and 1:1 line with ±1 unit range (dashed lines) are added.

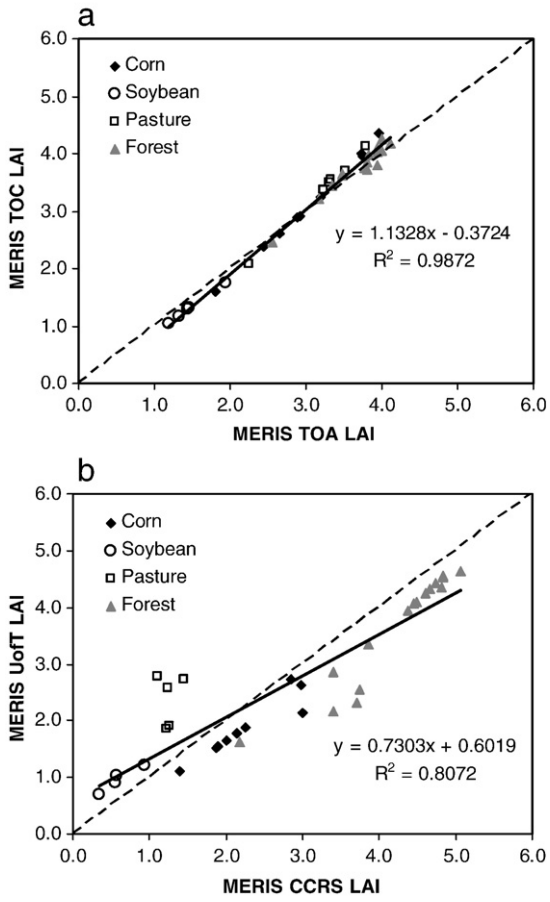

Fig. 7. Relation between (a) TOA and TOC LAI estimates and (b) CCRS and UofT LAI estimates. Linear regression (solid line) and 1:1 line (dashed line) are added.

3.2.4. Evaluation of MERIS LAI temporal consistency

Fig. 8 compares trajectories of TOA, TOC, CCRS LAI estimates during the 2008 growing season for pixels falling within the corn (CFIA_05) and soybean (CFIA_16) fields that were surveyed that year as well as a typical forest site (Forest ESU_05) and pasture site (CFIA_07) without coincident field measurements. In-situ reference estimates of LAI and L_e for pasture and forest sites, the corresponding 2006 survey date, are included. All three LAI estimates for corn are highly correlated (>98%) and showing typical growing pattern of corn (Fig. 8a). However all MERIS algorithms seem to agree with L_e rather than LAI when these in-situ quantities diverge later in the season. For soybean (Fig. 8b) CCRS LAI estimates shows good agreement with in-situ LAI while TOA and TOC algorithms overestimate the LAI for early growing stage with more open field and underestimate the LAI, tracking rather L_e, for peak growing season. Fig. 8c shows the temporal LAI pattern of a pasture filed and low LAI value in mid July is the harvesting time of that field. CCRS LAI estimates low value for pasture. Forest temporal LAI estimated using TOA LAI and TOC LAI algorithms are ~4 corresponding to the saturation level that we found in single date spatial evaluation. The CCRS LAI algorithm overestimated the forest values with larger scatter over time in comparison to the TOA and TOC retrievals.

4. Discussion

Both TOA and TOC LAI estimates exhibited similar spatial and temporal patterns and similar levels of agreement with in-situ based LAI and L_e estimates. Their lack of significant bias below 4 (LAI) is encouraging but this still translates into relative root mean square errors in excess of 25%. The saturation seen in their retrievals for in-situ LAI>4 may be related to the use of only landscape clumping within the simulations used to train both neural network retrieval algorithms. The landscape clumping is partly taken into account by considering mixed pixels as a fraction of pure vegetation or bare soil when simulating the vegetation surface reflectance at the pixel level (Bacour et al., 2006). Here, all of the targets show minimal landscape clumping so the retrieval should, and does, seem to correspond to in-situ based L_e rather than LAI for high LAI levels.

We also note that both TOA and TOC LAI estimates are very closely related (R^2>0.95 for linear regression) to MERIS NDVI (based on 620 nm and 754 nm wavebands). Thus, it is not clear how much additional information the multi-band algorithms are exploiting from MERIS in comparison to NDVI. As stated in Sridhar et al. (2008), the high correlation between MERIS NDVI and TOA LAI indicates the possibility to estimate LAI at early crop growth stages from MERIS data using simple empirical models. Furthermore, theories and empirical evidences support a relationship between NDVI and L_e (Leblanc, Chen, White, et al., 2005). It is possible that the TOA and TOC LAI algorithms therefore show reasonable agreement at lower LAI levels because LAI and L_e were also correlated ($R^2 = 0.7$) for these sites.

The lower performance of both the CCRS and UofT algorithms with MERIS data compared to previously published results with SPOT VGT products (Abuelgasim et al., 2006; Deng et al., 2006) may partially be explained by the exclusion of Short Wave Infra Red (SWIR) based vegetation indices, originally used in the SPOT VGT algorithms, due to the absence of SWIR bands with MERIS. However, CCRS and UofT algorithms also exhibited clear land cover specific biases. The increased agreement between satellite LAI and L_e over corn sites also suggests that these algorithms seem to be sensitive to clumping in a manner not well documented to date. A clumping correction is included in UofT algorithm based on the clumping index map. But the resolution and land cover dependency did not support well for the clumping correction for detail land use classes such as crop types.

At the same time we noticed that the SR does not exhibit an obvious saturation with LAI over forests in both CCRS and UofT algorithms. This has been documented for empirical datasets elsewhere over Canada (Fernandes et al., 2003) and suggests that broadleaf dominant forests in some Canadian landscapes tend to increase clumping with higher LAI so that the SR does not show saturation. However the estimated values are higher than in-situ LAI values and the variation is very much higher than other cover types. The variability may be due to their use of the SR that is known to have sensitivity to understory variability (Brown et al., 2000).

In this study detailed land cover information was used for CCRS LAI algorithm. However the deviation in the LAI estimates of pasture and forest indicate its land cover dependency. That is because of each function that is used to derive LAI is developed using the training data from a land cover subclass and may not be applicable for generalized land cover class.

5. Conclusion

MERIS LAI algorithms were evaluated against in-situ based LAI estimates over a region with varying land cover using MERIS FR data. TOA and TOC LAI estimates show differences of ~1 unit or 35% versus in-situ LAI. Both estimates showed saturation for higher (>4) LAI. The CCRS and UofT algorithms indicate land cover specific biases in their estimates that are related to the algorithm rather than the accuracy of the land cover for each evaluated pixel. This may be due to prior biases keyed to land cover including both conversions of spectral response functions for vegetation indices as well as retrieval of LAI given the input VI.

Our study shows limited single mid-growing season comparison however the evaluation of the temporal consistency of MERIS LAI estimates over a growing season for selected locations support our

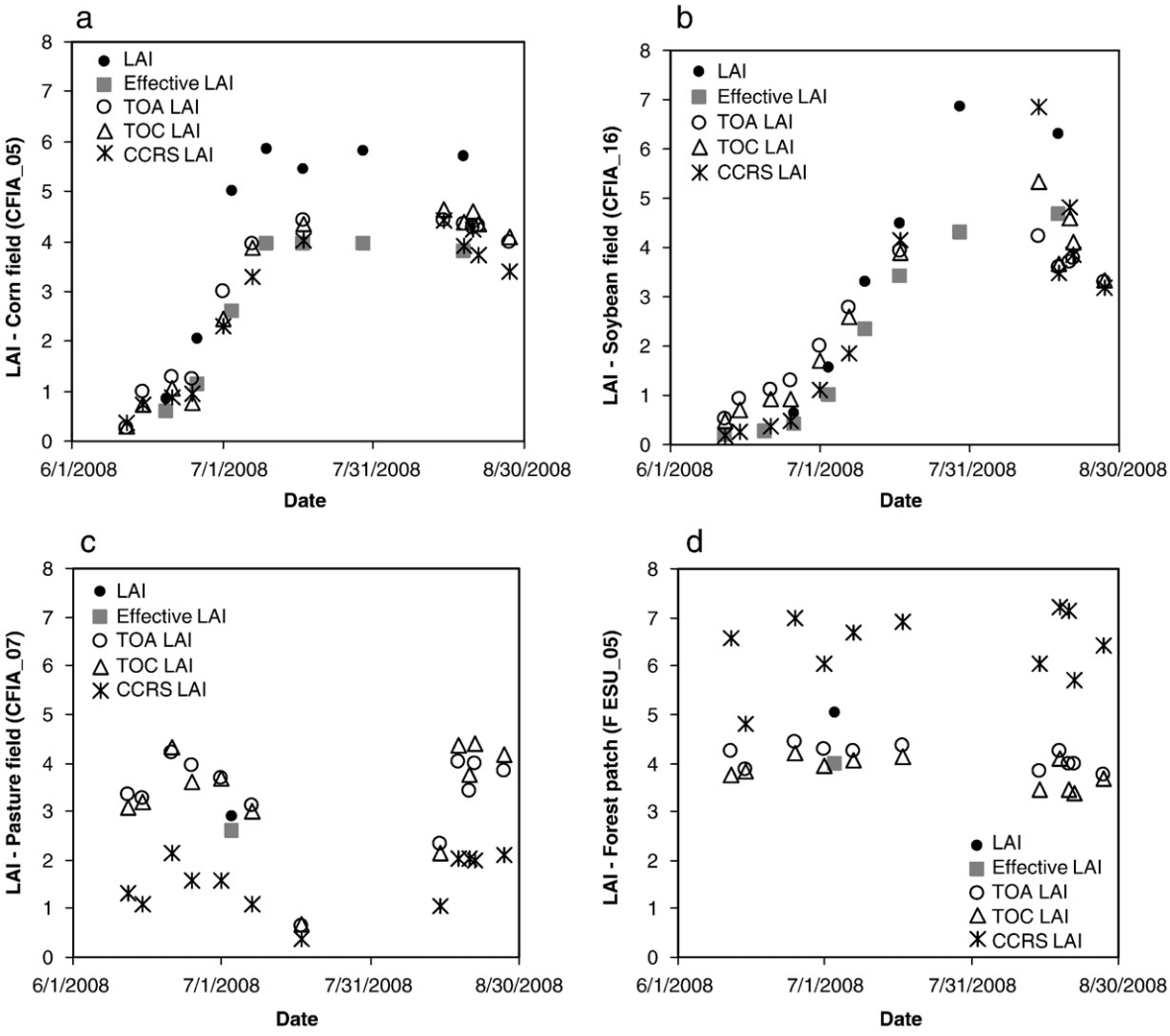

Fig. 8. Temporal consistency of TOA, TOC, and CCRS LAI estimates of (a) corn (b) soybean (c) pasture and (b) forest samples over the study area of 2008 growing season. In-situ LAI and L_e of corn and soybean (over 2008) and single in-situ LAI and L_e of pasture and forest (July 04, 2006) also shown as reference.

evaluation results. Clearly the significance of LAI both for GCOS requirements and for regional applications suggest that a standardized in-situ network of repeat measurements suitable for comparison with ~300 m resolution pixels be developed if we are also to meet the spatial representativeness requirement for Stage 3 validation (Morisette et al., 2006; Baret, et al., 2006b).

Our study suggests that, in the absence of regional in-situ LAI data for calibration, current MERIS TOA and TOC LAI retrieval algorithms (without clumping correction) are of limited use for widespread application over mixed land use landscapes similar to our study site. It seems that even some sort of clumping correction (e.g. using forest specific algorithms such as in the CCRS and UofT algorithms) resulted in lower agreements with in-situ based LAI than previously documented over with coarser resolution (500 m MODIS, 1 km SPOT VGT) estimates. The full resolution MERIS products enhances one's ability to relate LAI retrievals to location specific land management units (e.g. for crop monitoring) but we suggest that it may be time to explore the performance of MERIS LAI algorithms that take advantage of the substantial spectral sampling in the red edge region. Though TOA and TOC LAI algorithms use most of the MERIS bands within the visible and NIR range, they have not been specifically tuned to take into account mostly on the narrow band sampling of MERIS near the red edge that may provide robust LAI retrievals (Canisius & Fernandes, 2008; Mutanga & Skidmore, 2004; Haboudane et al., 2004; Clevers et al., 1994). In some sense, our current study therefore serves as a baseline against which LAI algorithms that exploit the full potential of MERIS' spectral sampling and enhanced spatial resolution, compared to most low to moderate resolution imaging spectrometers, can be judged.

Acknowledgment

This work was conducted within the Natural Resources Canada Groundwater Geoscience Programme and funded by the Canadian Space Agency Government Initiatives Research Project. MERIS data was provided by the European Space Agency and received by Canada Centre for Remote Sensing through funding from the Canadian Space Agency. We thank staff at Canada Centre for Remote Sensing and Agriculture Canada, Research Branch for in-situ data sets. Jing Chen thanks Beiping Zhang for her assistance in UofT LAI processing. The authors thank two internal reviewers and three anonymous reviewers for their constructive comments.

References

Abuelgasim, A. A., Fernandes, R. A., & Leblanc, S. G. (2006). Evaluation of National and Global LAI products derived from optical remote sensing instruments over Canada. *IEEE Transactions On Geoscience And Remote Sensing*, *44*(7), 1872−1884.

Bacour, C., Baret, F., Béal, D., Weiss, M., & Pavageau, K. (2006). Neural network estimation of LAI, fAPAR, fCover and LAI×Cab, from top of canopy MERIS reflectance data: Principles and validation. *Remote Sensing of Environment*, *105*, 313−325.

Brown, L., Chen, J. M., Leblanc, S. G., & Cihlar, J. (2000). A shortwave infrared modification to the simple ratio for LAI retrieval in boreal forests: An image and model analysis. *Remote Sensing of Environment*, *71*(1), 16−25.

Baret, F., Bacour, C., Beal, D., Weiss, M., Berthelot, B., & Regner, P. (2006b). *Report on the Algorithm Theoretical Basis Document for MERIS Top of Canopy Land Products (TOC_VEG)*. Contract ESA AO/1-4233/02/I-LG, 2006.

Baret, F., Morissette, J. T., Fernandes, R. A., Champeaux, J. L., Myneni, R. B., Chen, J., Plummer, S., Weiss, M., Bacour, C., Garrigues, S., & Nickeson, J. E. (2006a). Evaluation of the representativeness of networks of sites for the global validation and intercomparison of land biophysical products: Proposition of the CEOS-BELMANIP. *IEEE Transactions on Geoscience and Remote Sensing*, *44*, 1794−1803.

Baret, F., Pavageau, K., Beal, D., Weiss, M., Berthelot, B., & Regner, P. (2006c). *Report on the Algorithm Theoretical Basis Document for MERIS Top of Atmosphere Land Products (TOA_VEG)*. Contract ESA AO/1-4233/02/I-LG, 2006.

Butson, C., & Fernandes, R. A. (2004). A consistency analysis of surface reflectance and leaf area index retrieval of overlapping clear sky Landsat ETM + imagery. *Remote Sensing of Environment*, *89*, 369−380.

Canisius, F., & Chen, J. M. (2007). Retrieving forest background reflectance in a boreal region from Multi-angle Imaging SpectroRadiometer (MISR) data. *Remote Sensing of Environment*, *107*, 312−321.

Canisius, F., & Fernandes, R. (2008). *A narrow band NDVI for robust LAI retrieval independent of canopy chlorphyll concentration — test with MERIS.* 2nd *MERIS/(A) ATSR User Workshop*, 22–26 Sep 2008, Rome, Italy (ESA SP-666).

Chen, J. M., & Black, T. A. (1992). Defining leaf area index for non-flat leaves. *Plant Cell Environment*, *15*, 421−429.

Chen, J. M., Govind, A., Sonnentag, O., Zhang, Y., Barr, A., & Amiro, B. (2006). Leaf area index measurements at Fluxnet-Canada forest sites. *Agricultural and Forest Meteorology*, *140*, 257−268.

Chen, J. M., & Leblanc, S. G. (2001). Multiple-scattering scheme useful for geometric optical modeling. *IEEE Transactions on Geoscience and Remote Sensing*, *39*, 1061−1071.

Chen, J. M., Menges, C. H., & Leblanc, S. G. (2005). Global mapping of foliage clumping index using multi-angular satellite data. *Remote Sensing of Environment*, *97*, 447−457.

Clevers, J. G. P. W., Büker, C., van Leeuwen, H. J. C., & Bouman, B. A. M. (1994). A framework for monitoring crop growth by combining directional and spectral remote sensing information. *Remote Sensing of Environment*, *50*(2), 161−170.

Cohen, W. B., Maiersperger, T. K., Yang, Z., Gower, S. T., Turner, D. P., Ritts, W. D., Berterretche, M., & Running, S. W. (2003). Comparisons of land cover and LAI estimates derived from ETM + and MODIS for four sites in North America: A quality assessment of 2000/2001 provisional MODIS products. *Remote Sensing of Environment*, *88*(3), 233−255.

Delegido, J., Fernandez, G., Gandia, S., & Moreno, J. (2008). Retrieval of chlorophyll content and LAI of crops using hyperspectral techniques: application to PROBA/CHRIS data. *International Journal of Remote Sensing*, *29*(24), 7107−7127.

Demarez, V., Duthoit, S., Baret, F., Weiss, M., & Dedieu, G. (2008). Estimation of leaf area and clumping indexes of crops with hemispherical photographs. *Agricultural and Forest Meteorology*, *148*, 644−655.

Deng, F., Chen, J. M., Plummer, S., Chen, M., & Pisek, J. (2006). Algorithm for global leaf area index retrieval using satellite imagery. *IEEE Transactions on Geoscience and Remote Sensing*, *44*(8), 2219−2229.

Fernandes, R., Butson, C., Leblanc, S., & Latifovic, R. (2003). Landsat-5 TM and Landsat-7 ETM + based accuracy assessment of leaf area index products for Canada derived from SPOT-4 VEGETATION data. *Canadian Journal of Remote Sensing*, *29*(2), 241−258.

Fernandes, R. A., Miller, J. R., Chen, J. M., & Rubinstein, I. G. (2004). Evaluating image-based estimates of leaf area index in boreal conifer stands over a range of scales using high-resolution CASI imagery. *Remote Sensing of Environment*, *89*, 200−216.

Garrigues, S., Lacaze, R., Baret, F., Morisette, J. T., Weiss, M., Nickeson, J., Fernandes, R., Plummer, S., Shabanov, N. V., Myneni, R. B, Knyazikhin, Y., & Yang, W. (2008a). Validation and intercomparison of global Leaf Area Index products derived from remote sensing data. *Journal of Geophysical Research*, *113*, G02028, doi: 10.1029/2007JG000635.

Garrigues, S., Shabanov, N. V., Swanson, K., Morisette, J. T., Baret, F., & Myneni, R. B. (2008b). Intercomparison and sensitivity analysis of Leaf Area Index retrievals from LAI-2000, AccuPAR, and digital hemispherical photography over croplands. *Agricultural and Forest Meteorology*, *148*, 1193−1209.

GCOS. (2006). *Systematic Observation Requirements for Satellite-based Products for Climate. Report of United Nations Environment Programme*. GCOS-107, WMO/TD No. 1338.

Haboudane, D., Miller, J. R., Pattey, E., Zarco-Tejada, P. J., & Strachan, I. B. (2004). Hyperspectral vegetation indices and novel algorithms for predicting green LAI of crop canopies: Modeling and validation in the context of precision agriculture. *Remote Sensing of Environment*, *90*, 337−352.

Houborg, R., Soegaard, H., & Boegh, E. (2007). Combining vegetation index and model inversion methods for the extraction of key vegetation biophysical parameters using Terra and Aqua MODIS reflectance data. *Remote Sensing of Environment*, *106*, 39−58.

Iiames, J. S., Congalton, R., Pilant, A., & Lewis, T. (2008). Validation of an integrated estimation of loblolly pine (*Pinus taeda* L.) leaf area index (lai) using two indirect optical methods in the Southeastern United States. *Southern Journal of Applied Forestry*, *32*(3), 101−110.

Jacquemoud, S., & Baret, F. (1990). PROSPECT: A model of leaf optical properties spectra. *Remote Sensing of Environment*, *34*, 75−91.

Kaufman, Y. J., Tanré, D., Remer, L. A., Vermote, E. F., Chu, A., & Holben, B. N. (1997). Operational remote sensing of tropospheric aerosol over land from EOS moderate resolution imaging spectroradiometer. *Journal of Geophysical Research*, *102*, 17051−17067.

Lang, A. R. G., & Xiang, Y. (1986). Estimation of leaf area index from transmission of direct sunlight in discontinuous canopies. *Agricultural and Forest Meteorology*, *37*, 229−243.

López-Lozano, R., Baret, F., García de Cortázar-Atauri, I., Bertrand, N., & Casterad, M. A. (2009). Optimal geometric configuration and algorithms for LAI indirect estimates under row canopies: The case of vineyards. *Agricultural and Forest Meteorology*, *149*(8), 1307−1316.

Latifovic, R., Olthof, I., Pouliot, D., Beaubien, J., & Pavlic, G. (2005). Land Cover Map of Canada 2005, Canada Centre for Remote Sensing (CCRS), Earth Sciences Sector, NRCan, ESS Program: Understanding Canada from Space (UCS).

Leblanc, S. G., Chen, J. M., Fernandes, R., Deering, D. W., & Conley, A. (2005). Methodology comparison for canopy structure parameters extraction from digital hemispherical photography in boreal forests. *Agricultural and Forest Meteorology*, *129*, 187−207.

Leblanc, S. G., Chen, J. M., White, H. P., Latifovic, R., Lacaze, R., & Roujean, J. L. (2005). Canada-wide foliage clumping index mapping from multiangular POLDER measurements. *Canadian Journal of Remote Sensing*, *31*(5), 364−376.

LI-COR. (1992). LAI-2000 Plant Canopy Analyzer Instruction Manual. Lincoln, NE, USA: LICOR Inc.

Morisette, J. T., Baret, F., Privette, J. L., Myneni, R. B., Nickeson, J., Garrigues, S., Shabanov, N. V., Weiss, M., Fernandes, R., Leblanc, S., Kalacska, M., Sánchez-Azofeifa, G. A., Chubey, M., Rivard, B., Stenberg, P., Rautiainen, M., Voipio, P., Manninen, T., Pilant, A., Lewis, T., Iiames, J., Colombo, R., Meroni, M., Busetto, L., Cohen, W., Turner, D., Warner, E. D., Petersen, G. W., Seufert, G., & Cook, R. (2006). Validation of global moderate-resolution LAI Products: A framework proposed within the CEOS Land Product Validation subgroup. *IEEE Transactions on Geoscience and Remote Sensing*, *44*, 1804−1817.

Mutanga, O., & Skidmore, A. K. (2004). Narrow band vegetation indices overcome the saturation problem in biomass estimation. *International Journal of Remote Sensing*, *25*(19), 3999−4014.

Nikon Co., (2006). *Nikon CoolPix 8800 manual*, Nikon Corporation, Chiyoda-ku, Tokyo 100-83331, Japan.

Nilson, T. (1971). A theoretical analysis of the frequency gaps in plant stands. *Agricultural and Forest Meteorology*, *8*, 25−28.

Pattey, E., Strachan, I. B., Boisvert, J. B., Desjardins, R. L., & McLaughlin, N. B. (2001). Detecting effects of nitrogen rate and weather on corn growth using micrometeorological and hyperspectral reflectance measurements. *Agricultural and Forest Meteorology*, *108*, 85−99.

Pedersen, P., & Lauer, J. G. (2004). Soybean growth and development in various management systems and planting dates. *Crop Science*, *44*, 508−515.

Rahman, H., & Dedieu, G. (1994). SMAC: A simplified method for the atmospheric correction of satellite measurements in the solar spectrum. *International Journal of Remote Sensing*, *15*, 123−143.

Samain, O., (2006). Multi-sensor fusion of optical satellite data for the determination of surface biophysical parameters, PhD Thesis, University of Toulous, France.

Sridhar, V. N., Mahtab, A., & Navalgund, R. R. (2008). Estimation and validation of LAI using physical and semi-empirical BRDF models. *International Journal of Remote Sensing*, *29*(4), 1229−1236.

Strachan, I. B., Stewart, D. W., & Pattey, E. (2005). Determination of leaf area index in agricultural systems. In J. L. Hatfield, & J. M. Baker (Eds.), *Micrometeorology in Agricultural Systems, Agronomy Monograph No. 47 ASA-CSSA-SSSA. 179–198*.

Verhoef, W. (1984). Light scattering by leaf layers with application to canopy reflectance modeling: The SAIL model. *Remote Sensing of Environment*, *16*, 125−141.

Weiss, M., Baret, F., Smith, G. J., Jonckheere, I., & Coppi, P. (2004). Review of methods for in situ leaf area index (LAI) determination Part II. Estimation of LAI, errors and sampling. *Agricultural and Forest Meteorology*, *121*, 37−53.

Weiss, M., Baret, F., Garrigues, S., & Lacaze, R. (2007). LAI and fAPAR CYCLOPES global products derived from VEGETATION. Part 2: Validation and intercomparison with MODIS Collection 4 products. *Remote Sensing of Environment*, *110*(3), 317−331.

Welles, J. M., & Cohen, S. (1996). Canopy structure measurement by gap fraction analysis using commercial instrumentation. *Journal of Experimental Botany*, *47*(302), 1335−1342.

Wiegand, C. L., Gerbermann, A. H., Gallo, K. P., Blad, B. L., & Dusek, D. (1990). Multisite analyses of spectral-biophysical data for corn. *Remote Sensing of Environment*, *33*(1), 1−16.

Wilhelm, W. W., Ruwe, K., & Schlemmer, M. R. (2000). Comparison of three leaf area index meters in a corn canopy. *Crop Science*, *40*, 1179−1183.

Yang, W., Tan, B., Huang, D., Rautiainen, M., Shabanov, N. V., Wang, Y., Privette, J. L., Huemmrich, K. F., Fensholt, R., Sandholt, I., Weiss, M., Ahl, D. E., Gower, S. T., Nemani, R. R., Knyazikhin, Y., & Myneni, R. B. (2006). MODIS leaf area index products: From validation to algorithm improvement. *IEEE Transactions on Geoscience and Remote Sensing*, *44*(7), 1885−1898.

Zurita-Milla, R., Kaiser, G., Clevers, J. P. G. W., Schneider, W., & Schaepman, M. E. (2007). Spatial unmixing of MERIS Data for monitoring vegetation dynamics. *Envisat Symposium 2007, 23–27 April 2007, Montreux, Switzerland (ESA SP-636)*.

ID	Title	Pages
4460075	Comparison and evaluation of Medium Resolution Imaging Spectrometer leaf area index products across a range of land use	11